JACS
JOURNAL OF THE AMERICAN CHEMICAL SOCIETY

Communication

pubs.acs.org/JACS

Live-Cell Targeting of His-Tagged Proteins by Multivalent *N*-Nitrilotriacetic Acid Carrier Complexes

Ralph Wieneke,[†,§] Noemi Labòria,[†,§] Malini Rajan,[‡] Alina Kollmannsperger,[†] Francesco Natale,[‡] M. Cristina Cardoso,[‡] and Robert Tampé*[,†]

[†]Institute of Biochemistry, Goethe-University Frankfurt, Max-von-Laue-Str. 9, D-60438 Frankfurt am Main, Germany

[‡]Department of Biology, Technische Universität Darmstadt, Schnittspahnstr. 10, D-64287 Darmstadt, Germany

Supporting Information

ABSTRACT: Selective and fast labeling of proteins in living cells is a major challenge. Live-cell labeling techniques require high specificity, high labeling density, and cell permeability of the tagging molecule to target the protein of interest. Here we report on the site-specific, rapid, and efficient labeling of endogenous and recombinant histidine-tagged proteins in distinct subcellular compartments using cell-penetrating multivalent chelator carrier complexes. In vivo labeling was followed in real time in living cells, demonstrating a high specificity and high degree of colocalization in the crowded cellular environment.

Live-cell labeling and tracking of proteins with therapeutic relevance pose a significant challenge.[1−3] To understand the interplay of proteins and cellular pathways in cells, a range of fluorescent reporters have been explored. Live-cell labeling demands high specificity, high labeling density, and cell permeability of the tagging molecule to track the protein of interest (POI) in the crowded cellular environment at a protein concentration of 300 mg/mL.[4] Large efforts have been made to site-specifically incorporate chemical reporters such as small organic dyes, genetically encoded amino acids, or autofluorescent proteins to label, track, and manipulate specific targets.[5] Selective tools such as probe incorporation mediated by enzymes (PRIME)[6] and the fusion proteins SNAP,[7,8] CLIP,[9] and Halo[10] emphasize these efforts. Organic probes are preferred over autofluorescent proteins because of their significantly smaller size, superior quantum yield, photostability, and broader spectral range. Small tags, such as the tetracysteine tag,[11] the retro-Diels−Alder reaction of tetrazines with alkenes,[12,13] *N*-nitrilotriacetic acid (NTA),[14,15] or its multivalent derivative *tris*NTA have further contributed to the analysis of structure, function, and dynamics of proteins.[16] The (sub)nanomolar affinity of the *tris*NTA moiety toward His-tagged proteins enables the site-specific and stoichiometric labeling of POIs. In contrast to *mono*NTA, *tris*NTA offers kinetically stable binding while the small size of the *tris*NTA/His-tag interaction pair keeps the influence on the physiological function of the POI as low as possible.[17] Both properties are of special interest for super-resolution microscopy, single-molecule tracking, and other emerging techniques.[18,19] The *tris*NTA/His-tag interaction pair has unique potential for highly specific labeling of POIs in living cells and intracellular delivery of functional His-tagged proteins in vivo.[20] However, its poor cell permeability has limited its in vivo applications to date.

Several technologies have been established for the intracellular delivery of proteins, nucleic acids, therapeutic agents, or other chemical reporters to study and perturb biological networks.[21,22] Cell-penetrating peptides (CPPs) have often been used to target cytosolic proteins without harming the cell.[23,24] One of the first identified CPPs was the transactivator of transcription (TAT) of HIV-1, which is responsible for cellular uptake and translocation into the nucleus.[25,26] The basic domain of TAT ($_{49}$RKKRRQRRR$_{57}$) has been identified to be responsible for cell penetration.[27] Since then, the TAT sequence has been conjugated to other proteins to facilitate fast and efficient internalization. In addition to TAT, other CPPs have been identified, including polyarginines,[28] Penetratin,[29] Transportan,[30] and cyclic arginine-rich peptides.[31] The low cytotoxicity of CPPs and the high diversity of the delivered cargoes make them an attractive choice for intracellular delivery.[32] Here, we describe a cell-penetrating *tris*NTA/His$_6$-TAT$_{49-57}$ carrier complex to internalize fluorescent *tris*NTA moieties for the efficient and rapid intracellular targeting of His-tagged proteins in mammalian cells.

We non-covalently linked HIV TAT$_{49-57}$ to Ni(II)-loaded *tris*NTA by forming a stoichiometrically defined carrier complex. HIV TAT$_{49-57}$ (RKKRRQRRR) equipped with six N-terminal histidines separated by a short flexible GGGS linker (Scheme 1) was synthesized using solid-phase Fmoc chemistry [see the Supporting Information (SI)]. For sensitive detection, the *tris*NTA was modified with different fluorophores, e.g., ATTO565 or AlexaFluor 647 (AF647). After Ni(II) loading, the *tris*NTA/His$_6$-TAT$_{49-57}$ carrier complex was formed to deliver the fluorescent multivalent chelator into the cytosol and nucleus. Once there, the *tris*NTA preferentially bound to the His$_{10}$-POI and released the TAT$_{49-57}$ carrier peptide because of its higher affinity. As previously shown, the affinity of *tris*NTA toward a His$_{10}$-tagged protein is 10-fold higher (K_D = 0.1 nM) compared with a His$_6$ tag, but the complex stoichiometry remains 1:1.[16] This allows for efficient and rapid exchange of the *tris*NTA carrier complex in vivo.

Here we focused on two medically relevant proteins located in distinct cellular compartments. First, we selected the antigen

Received: July 10, 2014
Published: September 19, 2014

dx.doi.org/10.1021/ja5063357 | J. Am. Chem. Soc. 2014, 136, 13975−13978

Scheme 1. (a) Live-Cell Labeling of His-Tagged Proteins in Distinct Cellular Compartments Using a Cell-Penetrating Non-covalent *tris*NTA Carrier Complex Formed by (b) Fluorescent *tris*NTA and His_6-Tagged TAT_{49-57}

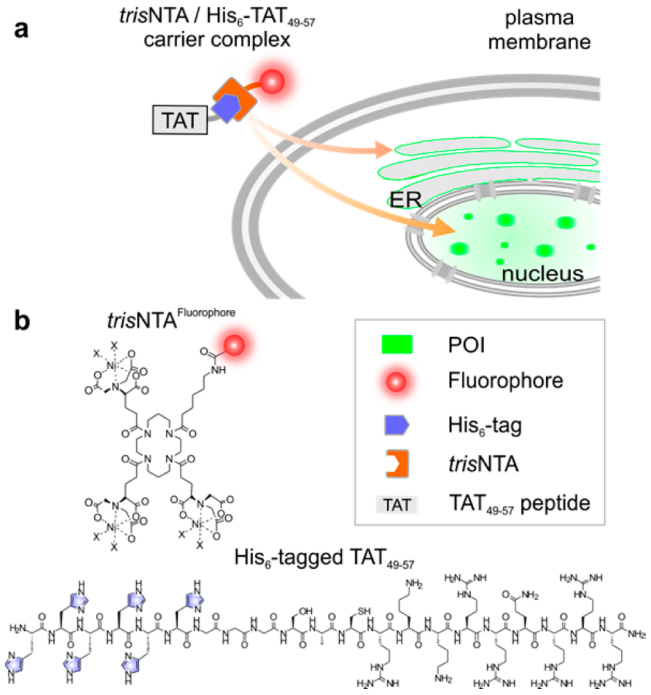

translocation complex TAP, which resides in the endoplasmic reticulum (ER) membrane. Within the adaptive immune response, TAP shuttles proteasomal degradation products into the ER for loading of major histocompatibility complex (MHC) class I molecules.[33] Second, the DNA-silencing complex methyl CpG binding protein 2 (MeCP2) localized in the nucleus was investigated. MeCP2 is known to bind to methylated DNA, and mutations in MeCP2 are linked to neurodevelopmental disorders (Rett syndrome).[34] For colocalization studies, both POIs were fused to an autofluorescent protein, TAP^{mVenus} and $MeCP2^{GFP}$.[35,36] Notably, MeCP2 harbors an endogenous sequence of seven consecutive histidines in an unstructured C-terminal region, whereas the TAP construct displays a recombinant C-terminal His_{10} tag.

First, human cervical cancer (HeLa) cells expressing membrane-bound $TAP1^{mVenus}$-His_{10} were fixed, permeabilized, and incubated with only 100 nM $trisNTA^{ATTO565}$ to target the His_{10}-tagged POI in the ER membrane. Confocal laser scanning microscopy revealed a perfect colocalization (Pearson coefficient 0.90) of the His_{10}-tagged TAP and $trisNTA^{ATTO565}$ (Figure S1 in the SI). Notably, cells that did not express $TAP1^{mVenus}$-His_{10} did not show any fluorescence signal in the $trisNTA^{ATTO565}$ channel, indicating the specificity of the intracellular labeling. Similar results were obtained for the MeCP2 construct (Figure S2). Here, C2C12 mouse myoblasts expressing $MeCP2^{GFP}$ in the nucleus were labeled with $trisNTA^{AF647}$ as noted above. Colocalization of the fluorescence signals emanating from both reporter dyes (GFP and AF647) was detected (Pearson 0.78), demonstrating the applicability of the *tris*NTA staining and full access of this internal naturally occurring His tag for subsequent live-cell labeling studies.

After demonstrating the site-specific labeling of His-tagged POIs in fixed cells, we carried out cellular uptake and colocalization studies in living cells. We anticipated that the *tris*NTA carrier complex would be taken up by cells and delivered *tris*NTA to the POI for labeling, as has been seen for other non-covalent TAT adducts. To address this, we performed in vivo labeling experiments of $TAP1^{mVenus}$-His_{10} and $MeCP2^{GFP}$ by tracing the uptake of the *tris*NTA/His_6-TAT_{49-57} carrier complex in living cells. HeLa cells expressing TAP^{mVenus}-His_{10} were incubated with 500 nM $trisNTA^{ATTO565}$/His_6-TAT_{49-57} carrier complex. After transduction for 1 h, site-specific labeling was imaged using confocal laser scanning microscopy. To facilitate the uptake of *tris*NTA/His_6-TAT_{49-57} in the nanomolar range, cells were preincubated with 0.25 mM chloroquine (1 h at 37 °C) prior to the transduction step. Chloroquine is an inhibitor of endosomal sequestration and is known to increase the transduction efficiency.[37] Representative images of the live-cell labeling of His_{10}-tagged TAP by complex formation with $trisNTA^{ATTO565}$ demonstrate specific ER staining (Figure 1; see Figure S3 for further examples).

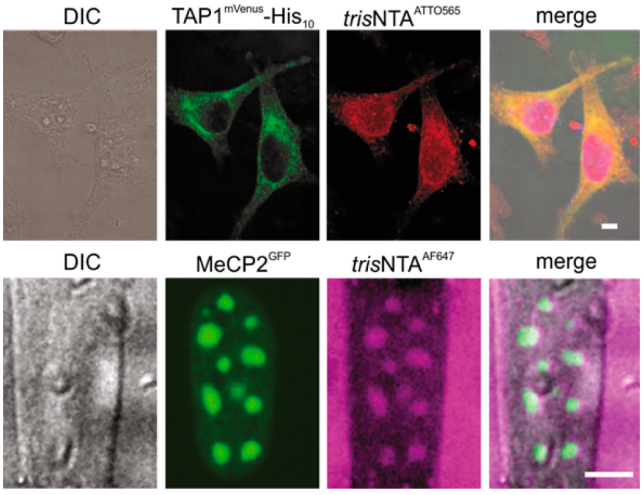

Figure 1. Live-cell labeling of His-tagged proteins by cell-penetrating *tris*NTA/His_6-TAT_{49-57} carrier complexes. $TAP1^{mVenus}$-His_{10}-transfected HeLa cells (upper row) and $MeCP2^{GFP}$-transfected C2C12 cells (lower row) were treated with the *tris*NTA carrier complex. Colocalization of $trisNTA^{fluorophore}$ (red/magenta) and the His-tagged POIs (green) was detected after cell incubation with the carrier complex for 60 min (TAP1) or 30 min (MeCP2). Site-specific recruitment of *tris*NTAs to the POI *via* complex formation was observed in the overlaid images (merged channel). See the SI for more examples. Scale bar: 5 μm.

Colocalization of the fluorescent signals for the His_{10}-tagged TAP1 and the red-emitting $trisNTA^{ATTO565}$ provided evidence for the site-specific and high-affinity labeling in living cells by the minimal lock-and-key element.

Similar results were obtained for the in vivo labeling of the transcription regulator $MeCP2^{GFP}$ (Figure 1). Transiently transfected C2C12 mouse myoblasts were incubated with the *tris*NTA/His_6-TAT_{49-57} carrier complex (9 μM) and the uptake was imaged 30 min after addition. In this case, the *tris*NTA was conjugated with an AF647 dye for readout. Merging the red channel of $trisNTA^{AF647}$ with the green channel of $MeCP2^{GFP}$ revealed colocalization of the small lock-and-key element and thus the site-specific targeting of the endogenous His-tag at heterochromatic regions of chromosomes (chromocenters). In all our live-cell approaches, strong ATTO565 or AF647 fluorescence of the *tris*NTA was observed that perfectly coincided with the fluorescence of the POI in the green

dx.doi.org/10.1021/ja5063357 | J. Am. Chem. Soc. 2014, 136, 13975−13978

channel (see the SI for further images). No colocalization of the *tris*NTA/His_6-TAT_{49-57} carrier complex was detected in cells expressing a TAP construct without the His tag or a truncated MeCP2 lacking the intrinsic heptahistidine sequence (Figure S4). It is important to note that no uptake of fluorescently labeled *tris*NTA was observed in the absence of the TAT_{49-57} carrier peptide (Figure S5) or in complex with a cumulative histidine sequence lacking the TAT_{49-57} peptide (His_5 peptide; Figure S6). In addition, the formation of the carrier complex is essential for cellular uptake, since no transduction of the *tris*NTAs was observed upon removal of the coordinated Ni(II) by addition of EDTA (Figure S7).

Finally, we followed the cellular uptake and labeling of POIs in real time by live-cell confocal microscopy. Imaging of $MeCP2^{GFP}$ in transiently transfected C2C12 cells and subsequent treatment with the preformed *tris*NTA/His_6-TAT_{49-57} carrier complex demonstrated rapid uptake within 10−30 min (Figure 2). Labeling of the cumulative histidines of

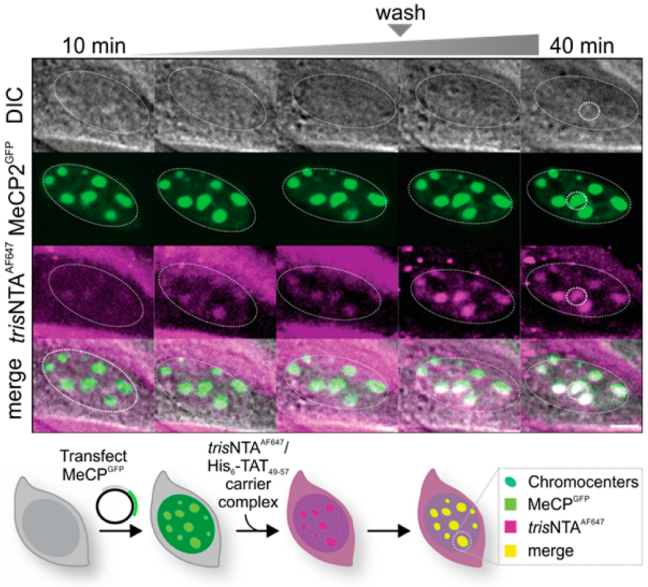

Figure 2. Site-specific targeting of $MeCP2^{GFP}$ by cell-penetrating *tris*NTA carrier complexes followed in real time. $MeCP2^{GFP}$ (green)-transfected C2C12 cells were treated with the *tris*NTA^{AF647}/His_6-TAT_{49-57} carrier complex and analyzed by live-cell microscopy. Colocalization of *tris*NTA^{AF647} (magenta) and $MeCP2^{GFP}$ was already detected after 10−30 min, demonstrating rapid and site-specific targeting of the POI by *tris*NTAs (merged channel). Scale bar: 5 μm.

MeCP2 proved to be fast and colocalization of the two fluorophores was already detected in the nucleus after 10 min. The two dyes accurately overlapped, indicating that our labeling approach enables efficient, rapid, and site-specific targeting of POIs in living cells. Notably, Ni(II) ions complexed to *tris*NTA at the given concentrations and incubation periods were nontoxic for the cells, as observed in long-term cell cultures and cell viability assays (Figure S8).

In summary, we have developed a TAT-mediated carrier system of fluorescent *tris*NTA for in vivo and real-time labeling of POIs harboring an endogenous or recombinant His-tag. This cell-penetrating *tris*NTA carrier system underwent rapid cellular uptake and showed site-specific labeling of His-tagged targets in distinct cellular compartments of living cells. Moreover, these studies prove the eminent potential for live-cell targeting of cumulative histidines by *tris*NTA groups, since the His tag is the smallest and one of the most frequently used tags for protein tagging and purification. This highly sensitive and rapid labeling method will have a great impact on live-cell imaging techniques, and we are currently investigating the use of this labeling method in super-resolution microscopy and in real-time tracking analysis of His-tagged targets within the interior of living cells.

■ ASSOCIATED CONTENT

Supporting Information

Methods, Figures S1−S8, and Schemes S1 and S2. This material is available free of charge *via* the Internet at http://pubs.acs.org.

■ AUTHOR INFORMATION

Corresponding Author

tampe@em.uni-frankfurt.de

Author Contributions

§R.W. and N.L. contributed equally.

Notes

The authors declare no competing financial interest.

■ ACKNOWLEDGMENTS

The German Research Foundation (Cluster of Excellence—Macromolecular Complexes, SFB807, SFB902, and SPP1623 to R.T. as well as GRK1657 and SPP1623 to M.C.C.) supported the work. We thank Christine Le Gal for editing the manuscript.

■ REFERENCES

(1) Marks, K. M.; Nolan, G. P. *Nat. Methods* **2006**, *3*, 591.
(2) Prescher, J. A.; Bertozzi, C. R. *Nat. Chem. Biol.* **2005**, *1*, 13.
(3) Sletten, E. M.; Bertozzi, C. R. *Angew. Chem., Int. Ed.* **2009**, *48*, 6974.
(4) Wombacher, R.; Cornish, V. W. *J. Biophotonics* **2011**, *4*, 391.
(5) Summerer, D.; Chen, S.; Wu, N.; Deiters, A.; Chin, J. W.; Schultz, P. G. *Proc. Natl. Acad. Sci. U.S.A.* **2006**, *103*, 9785.
(6) Uttamapinant, C.; Sanchez, M. I.; Liu, D. S.; Yao, J. Z.; Ting, A. Y. *Nat. Protoc.* **2013**, *8*, 1620.
(7) Keppler, A.; Gendreizig, S.; Gronemeyer, T.; Pick, H.; Vogel, H.; Johnsson, K. *Nat. Biotechnol.* **2003**, *21*, 86.
(8) Lukinavicius, G.; Umezawa, K.; Olivier, N.; Honigmann, A.; Yang, G.; Plass, T.; Mueller, V.; Reymond, L.; Correa, I. R., Jr.; Luo, Z. G.; Schultz, C.; Lemke, E. A.; Heppenstall, P.; Eggeling, C.; Manley, S.; Johnsson, K. *Nat. Chem.* **2013**, *5*, 132.
(9) Gautier, A.; Juillerat, A.; Heinis, C.; Correa, I. R., Jr.; Kindermann, M.; Beaufils, F.; Johnsson, K. *Chem. Biol.* **2008**, *15*, 128.
(10) Los, G. V.; Encell, L. P.; McDougall, M. G.; Hartzell, D. D.; Karassina, N.; Zimprich, C.; Wood, M. G.; Learish, R.; Ohana, R. F.; Urh, M.; Simpson, D.; Mendez, J.; Zimmerman, K.; Otto, P.; Vidugiris, G.; Zhu, J.; Darzins, A.; Klaubert, D. H.; Bulleit, R. F.; Wood, K. V. *ACS Chem. Biol.* **2008**, *3*, 373.
(11) Griffin, B. A.; Adams, S. R.; Tsien, R. Y. *Science* **1998**, *281*, 269.
(12) Blackman, M. L.; Royzen, M.; Fox, J. M. *J. Am. Chem. Soc.* **2008**, *130*, 13518.
(13) Devaraj, N. K.; Hilderbrand, S.; Upadhyay, R.; Mazitschek, R.; Weissleder, R. *Angew. Chem., Int. Ed.* **2010**, *49*, 2869.
(14) Guignet, E. G.; Hovius, R.; Vogel, H. *Nat. Biotechnol.* **2004**, *22*, 440.
(15) Orange, C.; Specht, A.; Puliti, D.; Sakr, E.; Furuta, T.; Winsor, B.; Goeldner, M. *Chem. Commun.* **2008**, 1217.
(16) Lata, S.; Reichel, A.; Brock, R.; Tampé, R.; Piehler, J. *J. Am. Chem. Soc.* **2005**, *127*, 10205.
(17) Lata, S.; Gavutis, M.; Tampé, R.; Piehler, J. *J. Am. Chem. Soc.* **2006**, *128*, 2365.

(18) Giannone, G.; Hosy, E.; Levet, F.; Constals, A.; Schulze, K.; Sobolevsky, A. I.; Rosconi, M. P.; Gouaux, E.; Tampé, R.; Choquet, D.; Cognet, L. *Biophys. J.* **2010**, *99*, 1303.
(19) Grunwald, C.; Schulze, K.; Giannone, G.; Cognet, L.; Lounis, B.; Choquet, D.; Tampé, R. *J. Am. Chem. Soc.* **2011**, *133*, 8090.
(20) June, R. K.; Gogoi, K.; Eguchi, A.; Cui, X. S.; Dowdy, S. F. *J. Am. Chem. Soc.* **2010**, *132*, 10680.
(21) Schwarze, S. R.; Ho, A.; Vocero-Akbani, A.; Dowdy, S. F. *Science* **1999**, *285*, 1569.
(22) Morris, M. C.; Deshayes, S.; Heitz, F.; Divita, G. *Biol. Cell* **2008**, *100*, 201.
(23) Heitz, F.; Morris, M. C.; Divita, G. *Br. J. Pharmacol.* **2009**, *157*, 195.
(24) Stewart, K. M.; Horton, K. L.; Kelley, S. O. *Org. Biomol Chem.* **2008**, *6*, 2242.
(25) Frankel, A. D.; Pabo, C. O. *Cell* **1988**, *55*, 1189.
(26) Tunnemann, G.; Martin, R. M.; Haupt, S.; Patsch, C.; Edenhofer, F.; Cardoso, M. C. *FASEB J.* **2006**, *20*, 1775.
(27) Vives, E.; Brodin, P.; Lebleu, B. *J. Biol. Chem.* **1997**, *272*, 16010.
(28) Wender, P. A.; Mitchell, D. J.; Pattabiraman, K.; Pelkey, E. T.; Steinman, L.; Rothbard, J. B. *Proc. Natl. Acad. Sci. U.S.A.* **2000**, *97*, 13003.
(29) Joliot, A.; Pernelle, C.; Deagostini-Bazin, H.; Prochiantz, A. *Proc. Natl. Acad. Sci. U.S.A.* **1991**, *88*, 1864.
(30) Pooga, M.; Soomets, U.; Hallbrink, M.; Valkna, A.; Saar, K.; Rezaei, K.; Kahl, U.; Hao, J. X.; Xu, X. J.; Wiesenfeld-Hallin, Z.; Hokfelt, T.; Bartfai, T.; Langel, U. *Nat. Biotechnol.* **1998**, *16*, 857.
(31) Lattig-Tunnemann, G.; Prinz, M.; Hoffmann, D.; Behlke, J.; Palm-Apergi, C.; Morano, I.; Herce, H. D.; Cardoso, M. C. *Nat. Commun.* **2011**, *2*, 453.
(32) Rothbard, J. B.; Garlington, S.; Lin, Q.; Kirschberg, T.; Kreider, E.; McGrane, P. L.; Wender, P. A.; Khavari, P. A. *Nat. Med.* **2000**, *6*, 1253.
(33) Parcej, D.; Tampé, R. *Nat. Chem. Biol.* **2010**, *6*, 572.
(34) Brero, A.; Leonhardt, H.; Cardoso, M. C. *Curr. Top. Microbiol. Immunol.* **2006**, *301*, 21.
(35) Parcej, D.; Guntrum, R.; Schmidt, S.; Hinz, A.; Tampe, R. *PLoS One* **2013**, *8*, No. e67112.
(36) Brero, A.; Easwaran, H. P.; Nowak, D.; Grunewald, I.; Cremer, T.; Leonhardt, H.; Cardoso, M. C. *J. Cell Biol.* **2005**, *169*, 733.
(37) Lee, C. M.; Tannock, I. F. *Br. J. Cancer* **2006**, *94*, 863.

Supporting Information

Live-cell targeting of His-tagged proteins by multivalent N-nitrilotriacetic acid carrier complexes

Ralph Wieneke[†,‡], Noemi Labòria[†,‡], Malini Rajan[#], Alina Kollmannsperger[†], Francesco Natale[#], M. Cristina Cardoso[#], Robert Tampé[*,†]

[†]Institute of Biochemistry, Biocenter, Goethe-University Frankfurt, Max-von-Laue-Str. 9, D-60438 Frankfurt/M., Germany

[#]Department of Biology, Technische Universität Darmstadt, Schnittspahnstr. 10, D-64287 Darmstadt, Germany

Table of Contents for Supporting Information

Abbreviations

aa, amino acid; Boc, *tert*-butyloxycarbonyl; CLSM, confocal laser-scanning microscopy; DAPI, 4',6-diamidino-2-phenylindole; DMEM, Dulbecco's modified eagle medium; DIPEA, *N*,*N*-diisopropylethylamine; EDT, 1,2-ethanedithiol; EDTA, ethylenediaminetetraacetic acid; ER, endoplasmic reticulum; FCS, fetal calf serum; Fmoc, 9-Fluorenylmethoxycarbonyl; GFP, green fluorescent protein; HBS, HEPES-buffered saline; HBTU, *o*-(Benzotriazol-1-yl)-*N*,*N*,*N*',*N*'-tetramethyluronium hexafluorophosphate; MeCP2, methyl CpG binding protein 2; Mmt, *para*-methoxytrityl; NHS, N-hydroxysuccinimide; NTA, nitrilotriacetic acid; SPPS, solid phase peptide synthesis; PBS, phosphate buffer saline; PEI, polyethyleneimine; *t*Bu, *tert*-butyl; RP-HPLC, reversed phase high-performance liquid chromatography; TAP, transporter associated with antigen processing; TAT, transactivator of transcription**;** TFA, trifluoroacetic acid; TIPS, triisopropylsilane; Trt, trityl; YFP, yellow fluorescent protein.

Materials and Methods

Peptides were synthesized using Fmoc-chemistry in a 0.1 mmol scale, assisted by microwave on a LIBERTY 1 Peptide Synthesizer (CEM). Fmoc-aa, HBTU, and Fmoc-Rink-Amide MBHA resin for SPPS were purchased form Iris Biotech. Fmoc-aa contained the following side chain protecting groups: Arg(Pbf), Cys(Mmt), Gln(Trt), His(Trt), Lys(Boc), and Ser(*t*Bu). AlexaFluor647 NHS-ester was obtained from Invitrogen and ATTO565 NHS-ester from ATTO-Tec GmbH. All reagents and solvents were of the highest analytical grade available, supplied by Fluka, Sigma-Aldrich, Merck, or Carl Roth, and were used without further purification. Cell culture materials were purchased from Sigma-Aldrich. Analytical HPLC analysis was conducted on a JASCO HPLC system equipped to a PerfectSil C4 analytical column (250 x 4.6 mm, 300 ODS, 5 µm, MZ-Analytical), a diode array detector, and using gradients starting from water with 0% methanol and increasing the hydrophobicity to 15% methanol as the mobile phase, both buffers containing 0.1% TFA. HPLC purification of the TAT_{49-57} peptide was performed using the same HPLC system and a C4 column connected to a fraction collector. The synthesis, dye labeling and Ni(II)-loading of *tris*NTA were performed as previously described.[1,2] All compounds were analyzed by MALDI-TOF-MS.

General procedures

Solid-phase peptide synthesis (SPPS)

All reaction steps were performed under microwave-irradiation using the Liberty 1 (CEM). The His_6-tagged TAT_{49-57} peptide was synthesized using standard coupling protocols for microwave-assisted SPPS. The molar excess of reagents was calculated with regard to resin substitution. *Fmoc-deprotection*: Fmoc-Rink-Amide MBHA resin was treated with 20% piperidine in DMF (1x 0.5 min, 1x 5 min, each 7.0 mL, 75 °C, 54 W), followed by washing with DMF (7.0 mL, 4x). *Coupling*: The resin was treated with Fmoc-aa (5 equiv.), HBTU (5 equiv.), and DiPEA (10 equiv.) in DMF (5.0 mL) for 30 min at RT and 15 min at 75 °C with a microwave power of 28 W, followed by washing with DMF (7.0 mL, 4x). To increase the yield, the coupling steps were repeated twice throughout the synthesis. *Cleavage and deprotection*: The resin was stirred with freshly prepared cleavage cocktail (95% TFA with phenol, TIPS, Milli-Q water, EDT, 1.25% each) for 4 h at RT. The TAT_{49-57} peptide was precipitated in ice-cold Et_2O (40 mL) and stored at least 15 min at -20 °C. After centrifugation at 3000 rpm for 10 min and decantation, the pellet was washed and centrifuged two more times with Et_2O (40 mL). The peptide was finally dissolved in *tert*-BuOH/H_2O (4/1, v/v), lyophilized, and purified by RP-HPLC using a gradient starting from water with 0% methanol and increasing the hydrophobicity to 15% methanol (both buffers containing 0.1% TFA) in 40 min at 1 mL/min on a C4 column. Retention time in RP-HPLC (column: PerfectSil C4), 28.0 min. MALDI-TOF-MS: m/z 2592.3 (calcd. for $(M - H)^-$: 2592.9 $C_{104}H_{173}N_{55}O_{23}S$).

Cell culture

Human cancer HeLa cells were cultured in DMEM supplemented with 10% FCS, 50 µg/mL gentamicin, and 2 mM glutamine. Mouse C2C12 myoblast cells were cultured in DMEM supplemented with 20% FCS, 50 µg/mL gentamicin and 2 mM glutamine.[3] The cell lines were incubated at 37 °C in a humidified atmosphere with 5% CO_2.

Plasmids and transfection

The plasmid encoding for human $TAP1^{mVenus}$-His_{10} and $TAP2^{mCerulean}$-strepII were previously described.[4] HeLa cells were transiently transfected with 18 mM of branched PEI with a DNA/PEI ratio of 1:3. Expression plasmid encoding human MeCP2 tagged with GFP and $MeCP2\Delta^{YFP}$ were previously described.[5] C2C12 cells were transfected using Amaxa (Lonza, Cologne, Germany) nucleofection kit (solution V, program B-032).[6] After 24 to 48 h, cells were either fixed and stained or used directly for live-cell labeling and imaging.

Cell viability assays

Trypan blue staining: Before fluorescence imaging, cells were washed with PBS and incubated with 0.04% Trypan blue in PBS at 37 °C for 2 min. Cells were rinsed three times with PBS and the cell morphology as well as cell viability were analyzed in the differential interference contrast (DIC) mode under the microscope. Dead cells were visualized by the appearance of a blue color.

SYTOX Blue exclusion assay: 0.3 x 10^6 cells were seeded in a six-well dish, grown and washed as described above. After 24 h, cells were washed with PBS and exposed to the *tris*NTA^{fluorophore}/His_6-TAT_{49-57} carrier complex, His_6-tagged TAT_{49-57}, and *tris*NTA^{fluorophore} (5 µM each) for 30 min at 37 °C. The cells were washed three times with PBS and cultured in DMEM supplemented with 10% FCS. The SYTOX Blue assay was performed at given time points (30 min and 5 h after transduction). After harvesting the cells by the addition of 0.5 mL 0.05% trypsin supplemented with 0.02% EDTA, the cells were centrifuged at 800 rpm for 5 min and resuspended in PBS to a cell concentration of 1.0 x 10^6 cells/ml. Prior to flow cytometry, the cell suspensions were incubated with 1 µM SYTOX Blue stain (Life Technologies) for 5 min and a minimum of 50.000 cells were analyzed with the Attune NxT Acuostic Cytometer (Life Technologies). Controls included a negative control (PBS treated cells) as well as a positive control, where cells were treated with 1 µg/mL listeriolysin for 5 min to lyse the cells. Cell viability was measured from the ratio of SYTOX Blue-positive cells/total number of cells.

Fluorescence microscopy with *tris*NTA^{fluorophore}

TAP1^{mVenus}-His$_{10}$ staining: Transiently transfected HeLa cells grown on cover slips were fixed 20 min with 4% formaldehyde in PBS at room temperature, quenched with 50 mM of glycine in PBS for 15 min, and permeabilized with 0.1% (v/v) Triton-X100 in PBS for 20 min. After blocking with bovine serum albumin (5% in PBS) for 60 min, cells were stained with 100 nM *tris*NTA^{ATTO565} followed by removal of excess *tris*NTA^{ATTO565} by washing with 5% bovine serum albumin (3x) and three times washing with PBS. Nuclei were visualized by DAPI staining and the cells were post-fixed with 2% formaldehyde for 10 min.

MeCP2^{GFP} staining: C2C12 cells transfected with MeCP2^{GFP} were grown on glass coverslips. 24 h after transfection, cells were fixed with 3.7% formaldehyde for 10 min and permeabilized with 0.5% (v/v) Triton X-100 for 20 min. Cells were then washed with PBS. 200 nM of *tris*NTA^{AlexaFluor647} diluted in PBS were added to the cells and incubated for 1 h at room temperature. After gentle removal of *tris*NTA by washing with PBS (3x), cells were post-fixed with 3.7% formaldehyde for 5 min. DNA was stained with DAPI followed by mounting in Mowiol 4-88 (Sigma-Aldrich).

Cellular uptake of *tris*NTA/His_6-TAT_{49-57} carrier complex

$TAP1^{mVenus}$-His_{10} *transfected cells*: 2 x 10^5 HeLa cells were seeded per well of an 8-well tissue culture chamber slide (Sarstedt) in culture medium and transiently transfected as described above. One day after transfection, cells were washed with PBS and exposed to 0.25 mM chloroquine in PBS for 1 h at 37 °C. After a brief PBS wash, the cells were incubated with 500 nM of the preformed complex between His_6-tagged TAT_{49-57} and *tris*$NTA^{ATTO565}$ (1:1) in PBS for 1 h in a CO_2 incubator, washed with DMEM supplemented with 10% FCS, and fixed with 4% paraformaldehyde for 20 min at RT. The cells were rinsed with PBS and immediately imaged with a Leica TCS SP5 microscope.

$MeCP2^{GFP}$ transfected cells: C2C12 cells transfected with $MeCP2^{GFP}$ were used for the live cell uptake experiments. A 1:1 ratio of *tris*NTA/His_6-TAT_{49-57} carrier complex was prepared by incubating His_6-tagged TAT_{49-57} and *tris*$NTA^{AlexaFluor647}$ (9 µM each) in HBS pH 7.5 for 40 min at room temperature. The complex was added to the cells. After 20 min, the solution was removed from the cells and washed subsequently with media. Live-cell uptake and co-localization was inspected with a Nikon Ti microscope.

Real-time uptake and His-tag targeting *via* fluorescently labeled *tris*NTA

$MeCP2^{GFP}$ transfected C2C12 cells were used for the real time uptake experiments. 9 µM of the preformed complex between His_6-tagged TAT_{49-57} and *tris*$NTA^{AlexaFluor647}$ (1:1) in HBS pH 7.5 was added to the cells. Immediately after addition, images were taken using the Ultra VIEW VoX spinning disc system (Perkin Elmer) with a Nikon Ti microscope equipped with an oil immersion Plan-Apochromat 60x/1.45 NA objective lens and connected to a humidified chamber. After 20 min, the solution was removed from the cells, washed with media and further inspected under the microscope.

Laser scanning microscopy

Confocal microscopic images were collected using an Ultra VIEW VoX spinning disc system (Perkin Elmer) with a Nikon Ti microscope equipped with an oil immersion Plan-Apochromat 60x/1.45 NA objective lens (pixel size in XY = 111 nm) or performed on a laser-scanning confocal microscope (Leica TCS SP5) using a Plan-Apochromat 63x/1.4 Oil DIC objective. Fluorophores were excited using 405 nm, 488 nm, 561 nm, and 633 nm lasers. Microscopes were enclosed by a chamber and kept at 37 °C in a humidified atmosphere with 5% CO_2 regulated by an ACU environmental control system from Olympus.

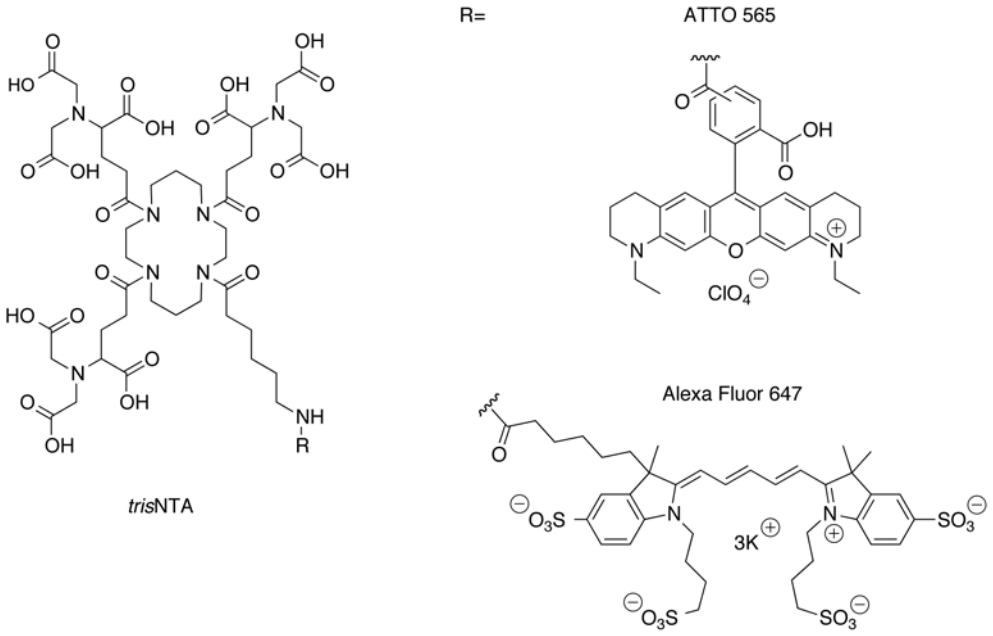

Scheme S1. Structures of *tris*NTA, ATTO565, and AlexaFluor647 used in this study.

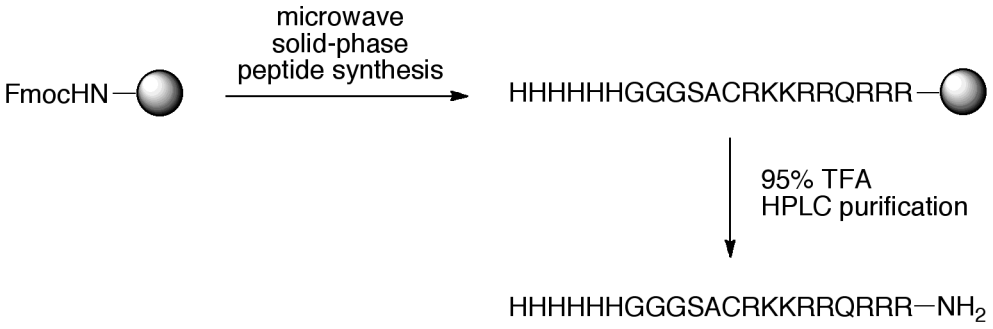

Scheme S2. Solid-phase peptide synthesis of His_6-tagged TAT_{49-57}.

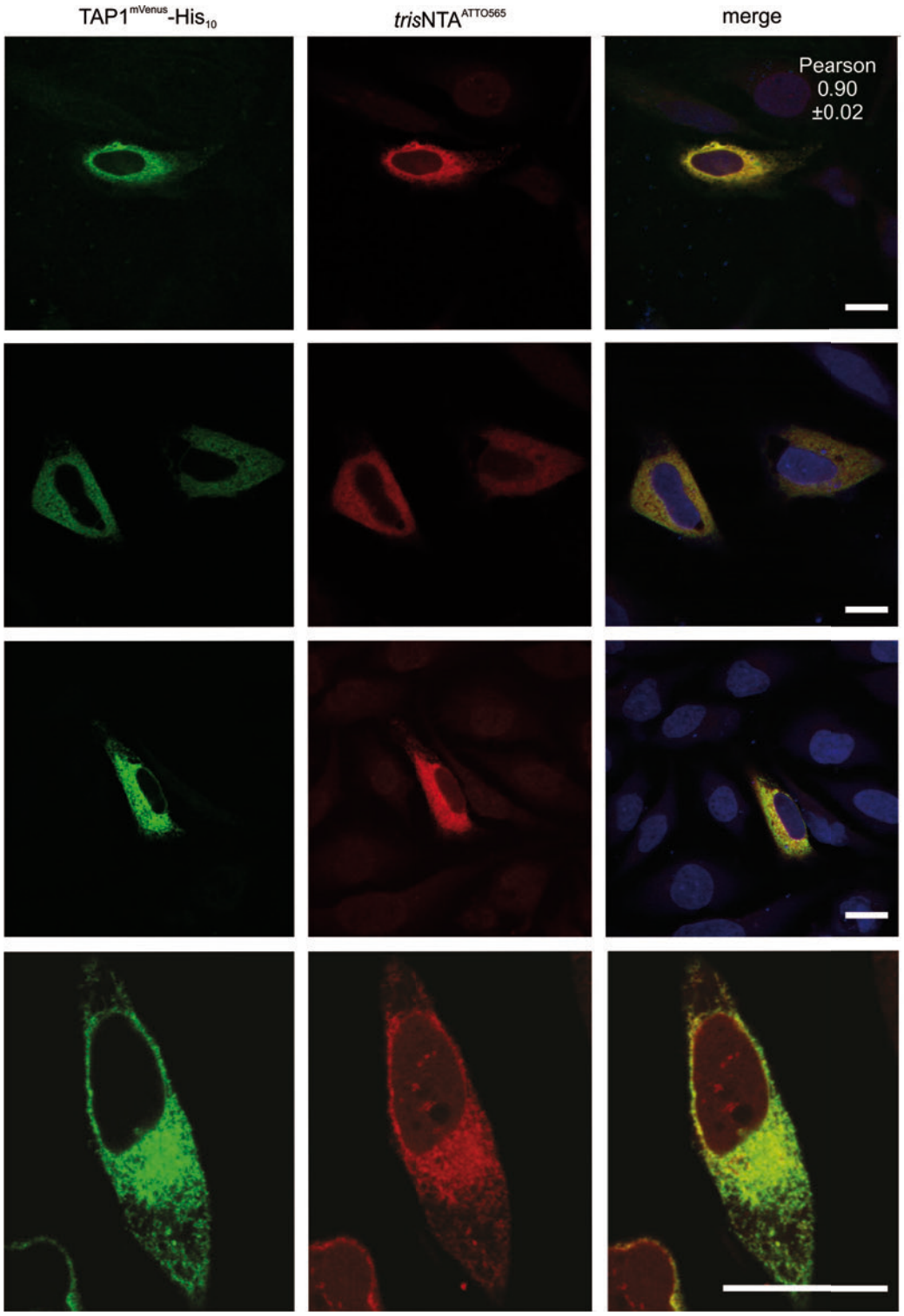

Figure S1. Fluorescent labeling of TAP1^{mVenus}-His$_{10}$ transfected HeLa cells. Co-localization of *tris*NTA^{ATTO565} (red channel) and His$_{10}$-tagged TAP1 (green channel) is only observed in cells expressing the fluorescent construct. Non-transfected cells (merged image, third row) show no fluorescence signal in the *tris*NTA^{ATTO565} channel, demonstrating a site-specific complex formation between *tris*NTA and the His-tagged POI. This verifies the high-specificity of the *tris*NTA-His-tag interaction for the *in vivo* labeling of His-tagged proteins. Nuclei were stained with DAPI (blue, merged channel). Scale bar: 20 µm.

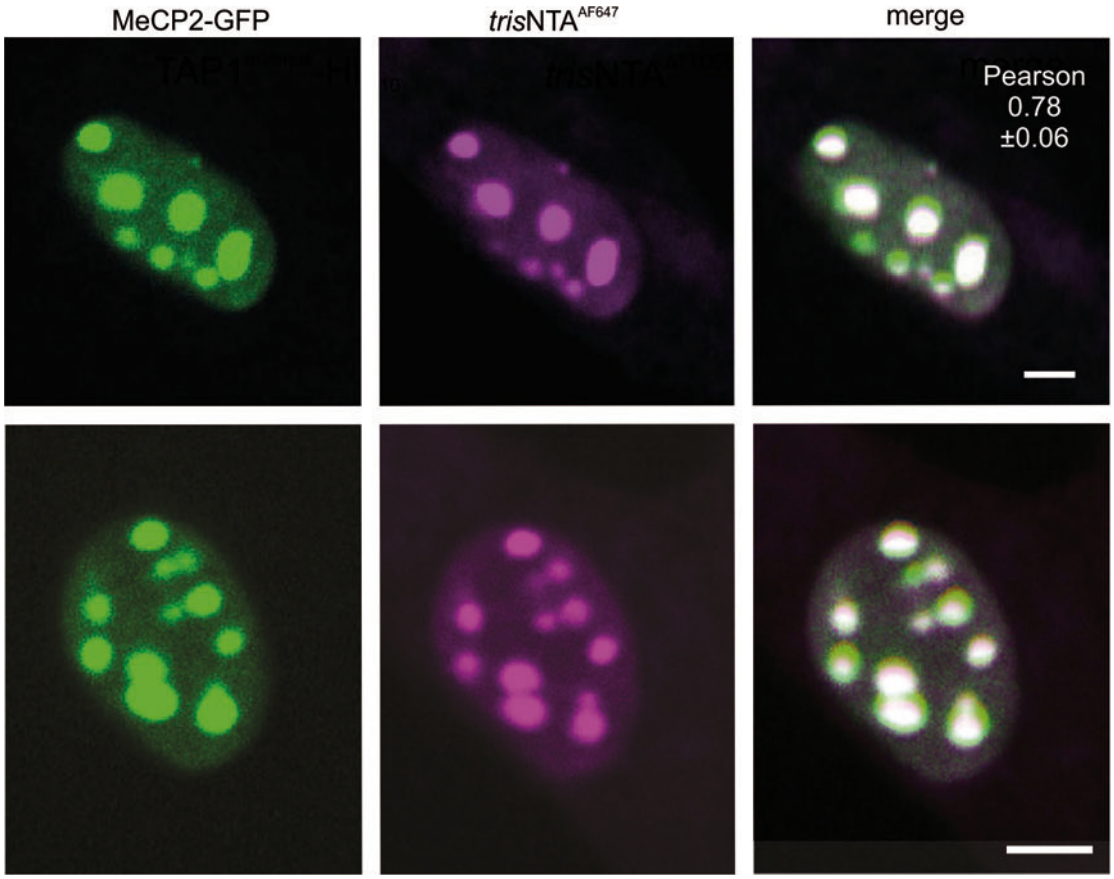

Figure S2. Fluorescent labeling of MeCP2^{GFP} transfected C2C12 cells. Co-localization of *tris*NTA^{AlexaFluor647} (purple channel) and MeCP2 (green channel) is only observed in the cell nucleus, whereas no unspecific binding of fluorescently labeled *tris*NTA in other cell compartments was detected. Scale bar: 5 µm.

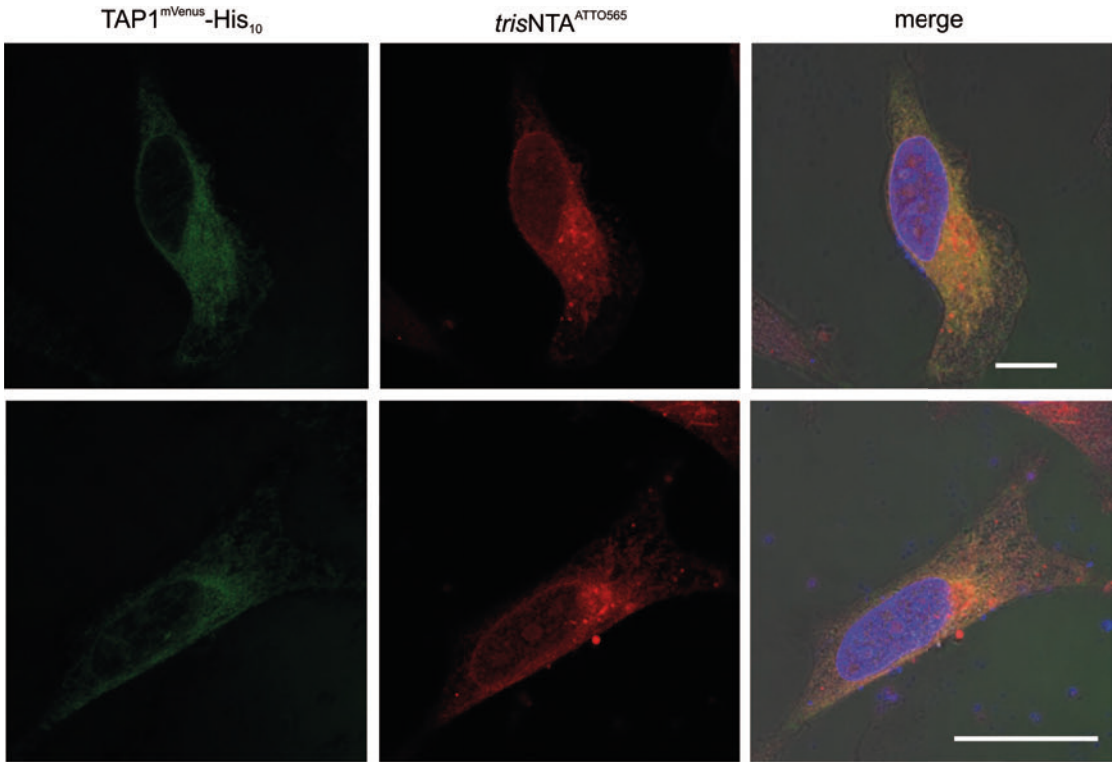

Figure S3. Live-cell protein labeling by *tris*NTA/His_6-TAT_{49-57} carrier complexes. $TAP1^{mVenus}$-His_{10} transfected HeLa cells were incubated with the *tris*$NTA^{ATTO565}$/His_6-TAT_{49-57} carrier complex (500 nM). Co-localization of *tris*$NTA^{ATTO565}$ (red channel) and the His-tagged $TAP1^{mVenus}$ (green channel) is detected after cell incubation with the carrier complex for 1 h at 37 °C. Site-specific recruitment of *tris*NTAs to the TAP1 construct *via* complex formation was detected in the overlaid images (merge channel). Scale bar: 25 µm.

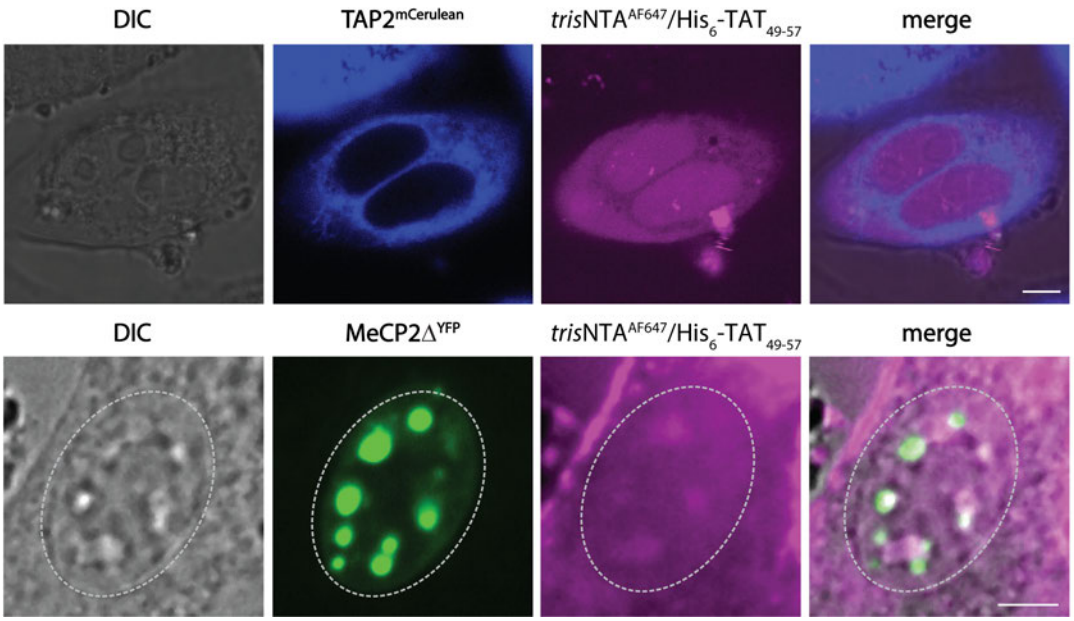

Figure S4. Live-cell uptake of *tris*NTA/His_6-TAT_{49-57} carrier complex in cells expressing POIs, which lack a fused or endogenous His-tag. $TAP2^{mCerulean}$-strepII transfected HeLa cells (upper row) and His-tag truncated $MeCP2\Delta^{YFP}$ transfected C2C12 cells (lower row) were incubated with the *tris*NTA^{AF647}/His_6-TAT_{49-57} carrier complex (10 μM). No co-localization of *tris*NTA^{AF647} (purple channel) and the $TAP2^{mCerulean}$ (upper row, blue channel) respectively $MeCP2\Delta^{YFP}$ (lower row, green channel) was detected after cell incubation with the carrier complex for 30 min at 37 °C, demonstrating the prerequisite of the His-tag for site-specific recruitment of *tris*NTA^{AF647}. In both cases, a cytosolic distribution of *tris*NTA^{AF647}/His_6-TAT_{49-57} carrier complex was observed. Scale bar: 5 μm.

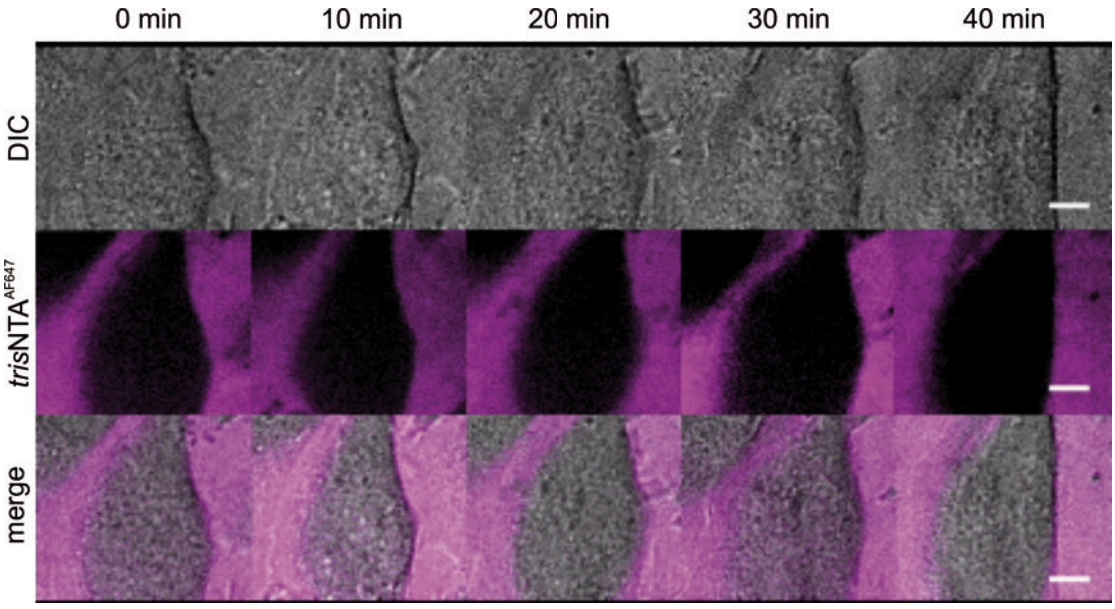

Figure S5. Real-time imaging of C2C12 cells in the presence of *tris*NTA^{AlexaFluor647} (9 µM). No unspecific uptake of dye-labeled *tris*NTA was observed in the time course of the experiment (40 min), confirming the dependency on the TAT_{49-57} mediated internalization of the small *lock-and-key* element. The morphology and shape of the cells is retained during the experiment, demonstrating the biocompatibility of the *tris*NTA for live-cell imaging and the high-affinity of the Ni(II) ions in complex with the multivalent chelator head *tris*NTA. Scale bar: 5 µm.

Figure S6. Confocal laser scanning images of TAP1^{mVenus}-His_{10} transfected HeLa cells treated with *tris*NTA^{ATTO565} in complex with a His_5-peptide. Cells were exposed 1 h to the preformed *tris*NTA^{ATTO565}/His_5 complex (500 nM each) at 37 °C in a humidified chamber and washed with 10% FCS in DMEM before imaging, identical as above mentioned for the carrier complex. No unspecific or endosomal uptake was detected, demonstrating that the intracellular delivery is strictly dependent on the TAT_{49-57} peptide. To assess cell viability in presence of the complex cells were stained by Trypan blue (merged channel). No significant increase in dead cell counts was observed as compared to mock-transfected cells. Scale bar: 25 µm.

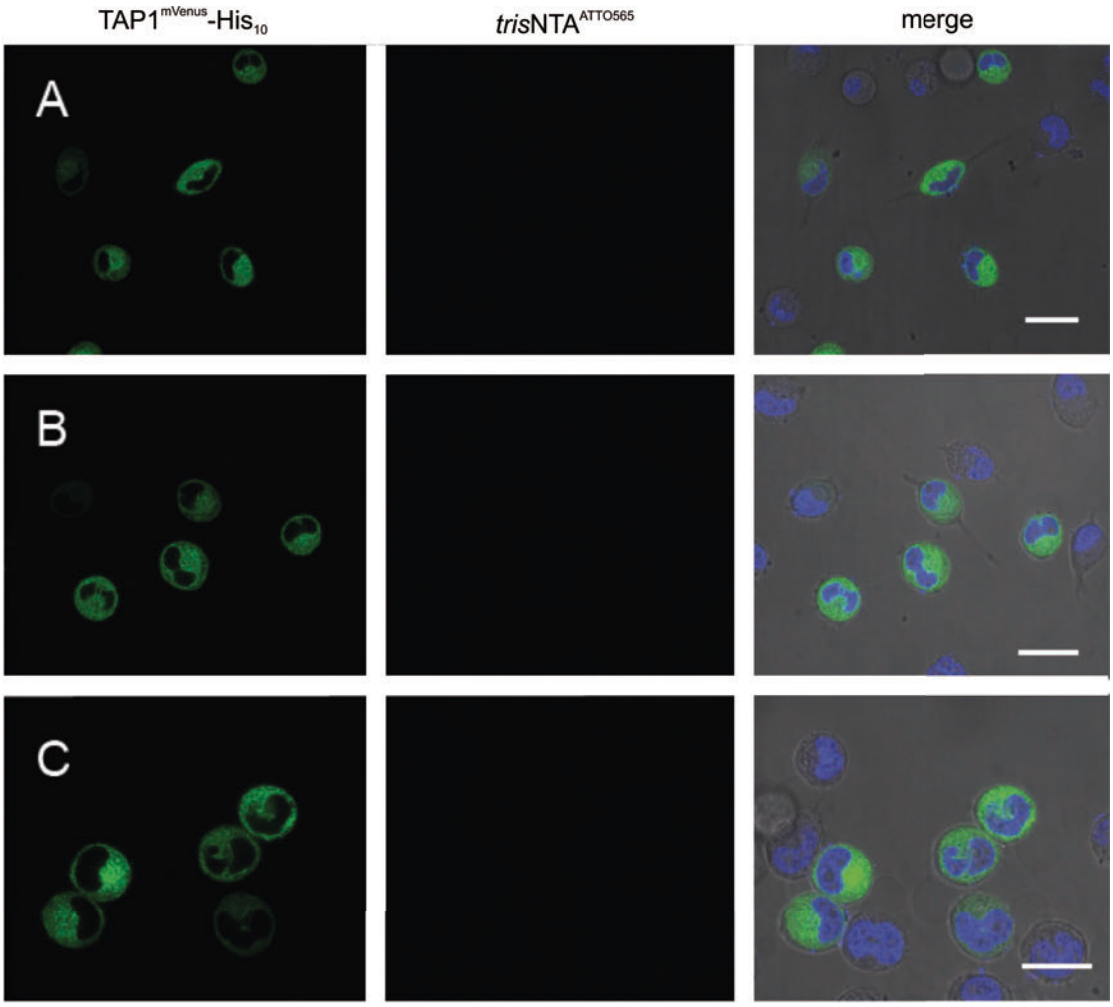

Figure S7. Influence of Ni(II) ions in cellular uptake of *tris*NTAs. *tris*NTA^{ATTO565} with and without His_6-tagged TAT_{49-57} (A and C, respectively) and with His_5 (B) were incubated in the presence of EDTA (1 mM) for 10 min at 37 °C. No signal corresponding to the fluorescence of *tris*NTA^{ATTO565} was detected in any of the cases. Samples were rinsed with PBS supplemented with 10% FCS. Nuclear staining is indicated by DAPI (blue). The concentration of fluorescently labeled *tris*NTA derivatives was 500 nM each. Scale bars: 25 µm.

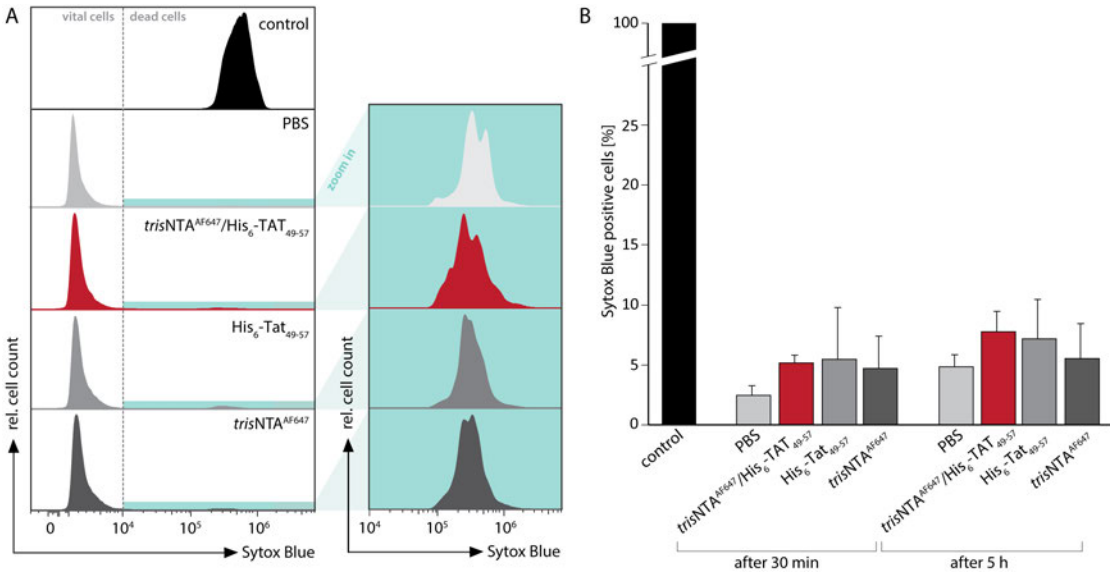

Figure S8. Cell viability assay of HeLa cells treated with *tris*NTA/His_6-TAT_{49-57} carrier complex. HeLa cells were incubated with *tris*NTA^{AF647}/His_6-TAT_{49-57} carrier complex, His_6-TAT_{49-57}, and *tris*NTA^{AF647} (5 μM each) for 30 min. Cell viability was assessed by the SYTOX Blue exclusion assay 0.5 h and 5 h after incubation (50.000 cells/experiment). Experiments are performed in triplicates. The mean and standard deviation is presented. A) Histograms of flow cytometry data show that only 6.3±0.8% and 6.6±5.2% of cells were stained by SYTOX Blue for *tris*NTA^{AF647}/His_6-TAT_{49-57} carrier complex as well as His_6-TAT_{49-57} treated cells. B) Bar diagrams demonstrate that 0.5 h and 5 h after transduction less then 10% of the cell population was stained by SYTOX Blue, proving that the delivery of *tris*NTA^{AF647}/ His_6-TAT_{49-57} is not deleterious to cells.

References

(1) Lata, S.; Reichel, A.; Brock, R.; Tampé, R.; Piehler, J. *J Am Chem Soc* **2005**, *127*, 10205.
(2) Labòria, N.; Wieneke, R.; Tampé, R. *Angew Chem Int Ed Engl* **2013**, *52*, 848.
(3) Yaffe, D.; Saxel, O. *Nature* **1977**, *270*, 725.
(4) Parcej, D.; Guntrum, R.; Schmidt, S.; Hinz, A.; Tampé, R. *PLoS One* **2013**, *8*, e67112.
(5) Agarwal, N.; Becker, A.; Jost, K. L.; Haase, S.; Thakur, B. K.; Brero, A.; Hardt, T.; Kudo, S.; Leonhardt, H.; Cardoso, M. C. *Hum Mol Genet* **2011**, *20*, 4187.
(6) Casas-Delucchi, C. S.; Brero, A.; Rahn, H. P.; Solovei, I.; Wutz, A.; Cremer, T.; Leonhardt, H.; Cardoso, M. C. *Nat Commun* **2011**, *2*, 222.